Mechanics of Advanced Composite Structures 4 (2017) 127-137

Semnan University

Mechanics of Advanced Composite Structures
journal homepage: http://MACS.journals.semnan.ac.ir

Free Vibration Analysis of Size-Dependent, Functionally Graded, Rectangular Nano/Micro-plates based on Modified Nonlinear Couple Stress Shear Deformation Plate Theories

K. Khorshidi [a,b*], A. Fallah [a]

[a] *Department of Mechanical Engineering, Arak University, Arak, Iran*
[b] *Institute of Nanosciences & Nanotechnolgy, Arak University, Arak, Iran*

PAPER INFO

Paper history:
Received 2016-12-17
Revised 2017-02-07
Accepted 2017-03-01

Keywords:
Rayleigh-Ritz
Vibration
Couple stress theory
Functionally graded

ABSTRACT

In the present study, a vibration analysis of functionally graded rectangular nano-/micro-plates was considered based on modified nonlinear coupled stress exponential and trigonometric shear deformation plate theories. Modified coupled stress theory is a non-classical continuum mechanics theory. In this theory, a material-length scale parameter is applied to account for the effect of nanostructure size that earlier classical plate theories are not able to explain. The material properties of the plate were assumed to vary according to a power-law form in the thickness direction. The governing equation of the motion of functionally graded, rectangular nano-/microplates with different boundary conditions were obtained based on the Rayleigh-Ritz method using complete algebraic polynomial displacement and rotation functions. The advantage of the present Rayleigh-Ritz method is that it can easily handle the different conditions at the boundaries of moderately thick rectangular plates (e.g., clamped, simply supported, and free). A comparison of the results with those available in the literature has been made. Finally, the effect of various parameters, such as the power-law index, thickness-to-length scale parameter ratio h/l, and aspect ratio a/b, on the natural frequency of nano/micro-plates are presented and discussed in detail.

DOI: 10.22075/MACS.2017.1800.1094

1. Introduction

The potential and applications of nano-/micro-materials in the development of technologies such as electronics, energy, environmental remediation, nano-/microsystem, medical and health, future transportation, etc. are important factors that encourage scientists to choose it for future projects. Today, scientists and engineers can reduce production costs, energy consumption, and maintenance with the aid of nanotechnology and its integration with other technologies. Also, using nano-/microtechnology has increased the durability of engineering structures.

Generally, size-dependent material models can be developed based on size-dependent continuum theories like classical couple stress theory [1], nonlocal elasticity theory [2], and strain gradient theory [3]. Couple stress theory is one of the higher-order continuum theories that contains material-length scale parameters and can cover the size effects of nano-/microstructures.

Functionally graded materials (FGMs) are heterogeneous composite materials in which the material properties vary continuously from one surface to the other surface. This is achieved by gradually varying the volume fraction of mixture materials. The merit of using these materials is that they can survive high thermal gradient environments. FGMs were first used as thermal barrier materials for aerospace structural applications and fusion reactors. Recently, they have been developed for general application as structural components in high-temperature environments [4]. Typically, an FGM is a mixture of ceramic and metal for the purpose of thermal protection against large temperature gradients. The ceramic material provides high-temperature resistance due to its low thermal conductivity, while the ductile metal prevents fracture due to its greater toughness. Because of the wide use of nano-/microplates in engineering applications, the study of functionally graded (FG), rectangular nano-/microplates has received considerable attention in recent years.

*Corresponding author, Tel.: +98-86-32625720 ; Fax: +98-86-34173450
E-mail address: k-khorshidi@araku.ac.ir

Matsunaga [5] analyzed the natural frequencies and buckling stresses of plates made of FG materials by taking into account the effects of transverse shear, normal deformations, and rotatory inertia. By expanding the power series of displacement components, a set of FG plates was derived using Hamilton's principle. Salehipour et al. [6] have developed a model for static and vibrating FG nano-/microplates based on the modified couple stress and three-dimensional elasticity theories. Ansari et al. [7] investigated the size-dependent vibrational behavior of FG, rectangular, Mindlin microplates, including geometrical nonlinearity. In their work, the FG Mindlin microplate was considered to be made of a mixture of metal and ceramic according to a power-law distribution. Kim and Reddy [8] have presented analytical solutions of a general third-order plate theory that accounts for the power-law distribution of two materials through thickness- and microstructure-dependent size effects. Thai and Vo [9] proposed a size-dependent model for the bending and free vibration of an FG plate based on the modified couple stress theory and sinusoidal shear deformation theory. Shaat et al. [10] developed a new Kirchhoff plate model using a modified couple stress theory to study the bending behavior of nanosized plates, including surface energy and microstructure effects. Lou and He [11] studied the nonlinear bending and free vibration responses of a simply supported, FG microplate lying on an elastic foundation within the framework of the modified couple stress theory, the Kirchhoff/Mindlin plate theory, and von Karman's geometric nonlinearity. He et al. [12] developed a new, size-dependent model for FG microplates by using the modified couple stress theory. Based on the strain gradient elasticity theory and a refined shear deformation theory, Zhang et al. [13] developed an efficient, size-dependent plate model to analyze the bending, buckling, and free vibration problems of FG microplates resting on an elastic foundation. Lou et al. [14] proposed a unified higher-order plate theory for FG microplates by adopting the modified couple stress theory to capture size effects and using a generalized shape function to characterize the transverse shear deformation. Thai and Kim [15] developed a size-dependent model of the bending and free vibration of an FG Reddy plate. Gupta et al. [16] presented an analytical model for the vibration analysis of partially cracked isotropic and FG, rectangular plates based on a modified couple stress theory. Li and Pan [17] developed a size-dependent, FG, piezoelectric microplate model based on the modified couple stress and sinusoidal plate theories. Nguyen et al. [18] studied the size-dependent behaviours of FG microplates using a novel quasi-3D shear deformation theory based on modified couple stress theory. Lei et al. [19] presented a size-dependent FG microplate model based on a modified couple stress theory requiring only one material-length scale parameter. Jandaghian and Rahmani [20] investigated the free vibration analysis of FG, piezoelectric-material, nanoscale plates based on Eringen's nonlocal Kirchhoff plate theory under simply supported–edge conditions. Şimşeka and Aydınc [21] considered the static bending and forced vibration of an imperfect FG microplate carrying a moving load based on Mindlin plate theory and the modified couple stress theory. Thai and Choi [22] presented an analytical solution for size-dependent models for the bending, buckling, and vibration of FG Kirchhoff and Mindlin plates based on modified couple stress theory. Khorshidi et al. [23], investigated the free vibrations of size-dependent, FG, rectangular plates with simply supported–boundary conditions based on nonlocal, exponential shear deformation theory using a Navier-type solution. Khorshidi and Fallah [24] analyzed the buckling response of FG, rectangular nanoplates with all edges simply supported based on nonlocal, exponential shear deformation theory according to Navier-type solutions. Khorshidi and Khodadadi [25] used a new, refined trigonometric shear deformation plate theory to study the out-of-plane vibration of rectangular, isotropic plates with different boundary conditions. Reddy and Kim [26] adopted a higher-order shear deformation theory to develop a size-dependent model for FG microplates. Simsek and Reddy [27] examined the bending and free vibration of microbeams based on various higher-order beam theories. Using first-order plate theory, Jung et al. [28, 29] investigated the buckling, static deformation, and free vibration of sigmoid, FG-material nano-/microplates embedded in a Pasternak elastic foundation.

The free vibration problem of plates can be solved using either the energy functional or the governing partial differential equations. Both can be taken by using standard analytical and numerical techniques. Among the techniques available are the finite element method [30], the boundary element method [31], the finite difference method [32], the differential quadrature method [33], the collocation method [34], the Galerkin method [35], and the Ritz method [36–39]. In this article, a modified couple stress theory according to the nonlinear exponential and trigonometric shear deformation theories was applied to analyze the free vibration of FG, rectangular nano-/microplates. The natural frequencies of the FG nano-/microplates were calculated using the Rayleigh-Ritz method based on minimizing the Rayleigh quotient. The novelty of the present paper is that the analytical solution was developed for size-dependent, FG, rectangular nano-/microplates using the modified nonlinear couple stress shear deformation theories for a combination of different boundary conditions (i.e., simply supported [S], clamped [C], and

free [F]), as follows: SSSS, SCSS, SCSC, SSSF, SFSF, SCSF, CCCC, SSCC, SCCC, CFCF, SSFF, CFSF, CFFF, SFCS, CFCC, SFCC, FFCC, CFCS, CSFF, SFFF, and FFFF. A comparison of the results with those available in the literature has been made. Finally, the effect of various parameters such as the power-law index, thickness-to-length scale parameter ratio (h/l), and aspect ratio (a/b) on the natural frequencies of nano-/microplates are presented and discussed in detail.

2. Governing Equation of Motion and Solution Procedure

Consider a size-dependent, rectangular nano-/microplate with uniform thickness h, length a, and width b made up of FG material as shown in Fig. 1. The properties of the nano-/microplate are assumed to vary through the thickness of the nanoplate according to a power-law distribution of the volume fractions of two materials between the two surfaces. The top surface ($x_3 = h/2$) of the size-dependent plate is fully ceramic, whereas the bottom surface ($x_3 = -h/2$) is fully metal. The plate regions are given by Eq. (1) as follows:

$$0 \le x_1 \le a, \quad 0 \le x_2 \le a, \quad -h/2 \le x_3 \le h/2. \tag{1}$$

where x_1, x_2, and x_3 are Cartesian coordinates. Poisson's ratio of the plate ϑ is assumed to be constant for ceramic and metal throughout the analysis.

Young's modulus and mass density are assumed to vary continuously through the plate thickness direction as

$$E(x_3) = (E_c - E_m)V(x_3) + E_m, \tag{2}$$

$$\rho(x_3) = (\rho_c - \rho_m)V(x_3) + \rho_m, \tag{3}$$

$$V(x_3) = \left(\frac{x_3}{h} + \frac{1}{2}\right)^g, \tag{4}$$

where the subscripts m and c represent the metallic and ceramic constituents, respectively; $\rho(x_3)$ is the plate density per unit area of the FG plate; $E(x_3)$ is the Young's modulus of the FG plate; $V(x_3)$ is the volume fraction; and g is the power-law index and takes only positive values.

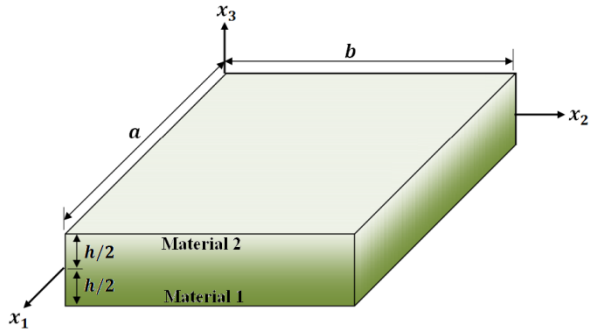

Figure 1. Rectangular plate geometry, dimensions, and coordinate system

According to Eqs. (2) and (3), when the power-law index g approaches zero or infinity, the plate is fully ceramic or metal, respectively. According to the following assumptions, the displacement field of the proposed plate theory is given as follows:

1. The displacement components u and v are the in-plane displacements in the x and y directions, respectively, and w is the transverse displacement in the z-direction. These displacements are small in comparison with the plate thickness.
2. The in-plane displacement u in the x direction and v in the y direction each consist of two parts.
   (a) A displacement component similar to displacement in classical plate theory.
   (b) A displacement component due to shear deformation, which is assumed to be exponential in exponential shear deformation theory and trigonometric in trigonometric shear deformation theory with respect to the thickness coordinate.
3. The transverse displacement w in the z direction is assumed to be a function of the x and y coordinates.

Based on the assumptions mentioned above, the displacement field can be described as

$$u(x_1, x_2, x_3, t) = u_0(x_1, x_2, x_3, t) - x_3 \frac{\partial w(x_1, x_2, t)}{\partial x_1} + f(x_3)\varphi_1(x_1, x_2, t), \tag{5}$$

$$v(x_1, x_2, x_3, t) = v_0(x_1, x_2, x_3, t) - x_3 \frac{\partial w(x_1, x_2, t)}{\partial x_2} + f(x_3)\varphi_2(x_1, x_2, t), \tag{6}$$

$$W(x_1, x_2, x_3, t) = w(x_1, x_2, t), \tag{7}$$

where, for exponential shear deformation plate theory, $f(x_3) = x_3 e^{-2\left(\frac{x_3}{h}\right)^2}$, and for trigonometric shear deformation plate theory, $f(x_3) = \frac{h}{\pi}\sin\left(\frac{\pi x_3}{h}\right)$ [23–25]. Also u, v, and W are the displacement in the x_1, x_2, and x_3 directions, respectively; u_0 and v_0 are the mid-plane displacements; and φ_1 and φ_2 are the rotation functions. With the assumed linear von Karman strain, the displacement-strain field will be as follows [22]:

$$\varepsilon_{11} = \frac{\partial u}{\partial x_1} = \frac{\partial u_0}{\partial x_1} - x_3 \frac{\partial^2 w}{\partial {x_1}^2} + f(x_3)\frac{\partial \varphi_1}{\partial x_1}, \tag{8}$$

$$\varepsilon_{22} = \frac{\partial v}{\partial x_2} = \frac{\partial v_0}{\partial x_2} - x_3 \frac{\partial^2 w}{\partial {x_2}^2} + f(x_3)\frac{\partial \varphi_2}{\partial x_2}, \tag{9}$$

$$\gamma_{12} = \frac{\partial u}{\partial x_2} + \frac{\partial v}{\partial x_1} = \frac{\partial u_0}{\partial x_2} + \frac{\partial v_0}{\partial x_1} - 2x_3 \frac{\partial^2 w}{\partial x_1 \partial x_2} + f(x_3)\left(\frac{\partial \varphi_1}{\partial x_2} + \frac{\partial \varphi_2}{\partial x_1}\right), \tag{10}$$

$$\gamma_{13} = \frac{\partial u}{\partial x_3} + \frac{\partial w}{\partial x_1} = \frac{df(x_3)}{dx_3}\varphi_1, \tag{11}$$

$$\gamma_{23} = \frac{\partial v}{\partial x_3} + \frac{\partial w}{\partial x_2} = \frac{df(x_3)}{dx_3}\varphi_2. \tag{12}$$

In the Eqs. (8–12), ε_{ii} are normal strains and γ_{ij} are shear strains. Considering Hooke's law for stress fields, the normal stress σ_{33} is assumed to be negligible in comparison within plane stresses σ_{11} and σ_{22}. Thus, the stress-strain relationship will be as follows:

$$\sigma_{11} = \frac{E(x_3)}{1-\vartheta^2}(\varepsilon_{11} + \vartheta\varepsilon_{22}) = \frac{E(x_3)}{1-\vartheta^2}\Big[f(x_3)\Big(\frac{\partial\varphi_1}{\partial x_1} + \vartheta\,\frac{\partial\varphi_2}{\partial x_2}\Big) + \Big(\frac{\partial u_0}{\partial x_1} + \vartheta\,\frac{\partial v_0}{\partial x_2}\Big) - x_3\frac{\partial^2 w}{\partial {x_1}^2} + \vartheta\,\frac{\partial^2 w}{\partial {x_2}^2}\Big], \quad (13)$$

$$\sigma_{22} = \frac{E(x_3)}{1-\vartheta^2}(\varepsilon_{22} + \vartheta\varepsilon_{11}) = \frac{E(x_3)}{1-\vartheta^2}\Big[f(x_3)\Big(\frac{\partial\varphi_2}{\partial x_2} + \vartheta\,\frac{\partial\varphi_1}{\partial x_1}\Big) + \Big(\frac{\partial v_0}{\partial x_2} + \vartheta\,\frac{\partial u_0}{\partial x_1}\Big) - x_3\frac{\partial^2 w}{\partial {x_2}^2} + \vartheta\,\frac{\partial^2 w}{\partial {x_1}^2}\Big], \quad (14)$$

$$\tau_{12} = G\gamma_{12} = \frac{E(x_3)}{2(1+\vartheta)}\left(\frac{\partial u_0}{\partial x_2} + \frac{\partial v_0}{\partial x_1} - 2x_3\frac{\partial^2 w}{\partial x_1 \partial x_2} + f(x_3)\Big(\frac{\partial\varphi_1}{\partial x_2} + \frac{\partial\varphi_2}{\partial x_1}\Big)\right), \quad (15)$$

$$\tau_{13} = \mathrm{G}(x_3)\gamma_{13} = \frac{\mathrm{E}(x_3)}{2(1+\vartheta)}\Big(\frac{\mathrm{df}(x_3)}{\mathrm{d}x_3}\varphi_1\Big), \quad (16)$$

$$\tau_{23} = \mathrm{G}(x_3)\gamma_{23} = \frac{\mathrm{E}(x_3)}{2(1+\vartheta)}\Big(\frac{\mathrm{df}(x_3)}{\mathrm{d}x_3}\varphi_2\Big), \quad (17)$$

where $\mathrm{G}(x_3) = \mathrm{E}(x_3)/(2(1+\vartheta))$ is the shear modulus of the plate.

In the modified couple stress theory, the strain energy of a linearly elastic continuum body on volume ∀ is defined by a function of both strain tensor and curvature tensor as

$$U_{max} = \frac{1}{2}\int_{\forall}(\sigma_{11}\varepsilon_{11} + \sigma_{22}\varepsilon_{22} + \sigma_{12}\gamma_{12} + \sigma_{13}\gamma_{13} + \sigma_{23}\gamma_{23} + m_{11}\chi_{11} + m_{22}\chi_{22} + m_{33}\chi_{33} + 2m_{12}\chi_{12} + 2m_{13}\chi_{13} + 2m_{23}\chi_{23})d\forall, \quad (18)$$

where σ_{ij}, ε_{ij}, and γ_{ij} are the components of the stress, normal strains, and shear strain tensors, respectively [1]. Also, m_{ij} are the components of the deviatoric part of the symmetric couple stress tensor, and χ_{ij} are the components of the symmetric curvature tensor defined by

$$\chi_{ij} = \frac{1}{2}\Big(\frac{\partial\theta_i}{\partial x_j} + \frac{\partial\theta_j}{\partial x_i}\Big),\ i,j = 1,2,3, \quad (19)$$

$$m_{ij} = \frac{E(z)}{1+\vartheta}l^2\chi_{ij}, \quad (20)$$

where l is the length scale parameter, and θ_i are the components of the rotation vector related to the displacement field. These are defined as follows:

$$\theta_1 = \frac{1}{2}\Big(\frac{\partial w}{\partial x_2} - \frac{\partial v}{\partial x_3}\Big), \quad (21)$$

$$\theta_2 = \frac{1}{2}\Big(\frac{\partial u}{\partial x_3} - \frac{\partial w}{\partial x_1}\Big), \quad (22)$$

$$\theta_3 = \frac{1}{2}\Big(\frac{\partial u}{\partial x_3} - \frac{\partial w}{\partial x_1}\Big). \quad (23)$$

The kinetic energy of the FG nano-/microplate is defined as follows:

$$\mathrm{T}_{max} = \frac{1}{2}\int_{\mathrm{v}}\rho(x_3)(\dot{\mathrm{u}}^2 + \dot{\mathrm{v}}^2 + \dot{\mathrm{w}}^2)\mathrm{d}\forall, \quad (24)$$

where the dot-top index contract indicates the differentiation with respect to the time variable.

In this section, the Rayleigh-Ritz method is employed to analyze the free vibration of the FG, rectangular nano-/microplates using coupled stess theory. In the Rayleigh-Ritz method, the admissible trial displacement and rotation functions can be introduced as follows [34]:

$$u_0 = \tilde{f}_1(x_1,x_2)\sum_{r=1}^{N_1}\sum_{s=1}^{r}u_n\,{x_1}^r{x_2}^{(r-s)}e^{i\omega_n t}, \quad (25)$$

$$v_0 = \tilde{f}_2(x_1,x_2)\sum_{r=1}^{N_1}\sum_{s=1}^{r}v_n\,{x_1}^r{x_2}^{(r-s)}e^{i\omega_n t}, \quad (26)$$

$$w = \tilde{f}_3(x_1,x_2)\sum_{r=1}^{N_1}\sum_{s=1}^{r}w_n\,{x_1}^r{x_2}^{(r-s)}e^{i\omega_n t}, \quad (27)$$

$$\varphi_1 = \tilde{f}_4(x_1,x_2)\sum_{r=1}^{N_1}\sum_{s=1}^{r}\varphi_{1_n}\,{x_1}^r{x_2}^{(r-s)}e^{i\omega_n t}, \quad (28)$$

$$\varphi_2 = \tilde{f}_5(x_1,x_2)\sum_{r=1}^{N_1}\sum_{s=1}^{r}\varphi_{2_n}\,{x_1}^r{x_2}^{(r-s)}e^{i\omega_n t}, \quad (29)$$

where u_n, v_n, w_n, φ_{1_n}, and φ_{2_n} are the generalized constant coefficients of the admissible trial functions; ω_n is the natural frequency of the plate; $i = \sqrt{-1}$ is the imaginary number; N_1 is the order of approximation; and $\tilde{f}_n(x_1,x_2), n = 1,2,3,4,5$ are the fundamental functions. The fundamental functions of the moderately thick, FG, rectangular nano-/microplates that satisfy the geometric boundary conditions are introduced as

$$\tilde{f}_n = {x_1}^{\alpha_1}{x_2}^{\alpha_2}(x_1-a)^{\alpha_3}(x_1-b)^{\alpha_4}. \quad (30)$$

The fundamental functions for different boundary conditions of the moderately thick, FG, rectangular nano-/microplates that were considered in the present study are listed in Table 1. In the Rayleigh-Ritz approach, the Lagrangian function of the system is given as

$$\Pi = U_{max} - T_{max}. \quad (31)$$

With the application of the Rayleigh-Ritz minimization method, the eigenvalue equation can be derived from Eq. (32).

$$\frac{\partial\Pi}{\partial q_i} = 0, \quad (32)$$

where $q_i = [u_i, v_i, w_i, \varphi_{1_i}, \varphi_{2_i}]^T$ is the vector of generalized coordinates and contains an unknown, undetermined coefficient. Eq. (32) can be written in matrix form as below:

$$([\mathrm{K}] - \omega_{\mathrm{n}}^2[\mathrm{M}])q_i = 0, \quad (33)$$

where

$$[\mathrm{K}] = \frac{\partial^2 U_{max}}{\partial q_i \partial q_j},\ [\mathrm{M}] = \frac{\partial^2 T_{max}}{\partial q_i \partial q_j}, \quad (34)$$

[K] is the stiffness matrix, and [M] is the mass matrix. This eigenvalue problem is solved to obtain the natural frequency parameters and vibration modal shapes of the FG, rectangular nano-/microplate.

Table 1. Fundamental functions of the admissible trial displacement and rotation functions for different combinations of boundary conditions

Boundary Conditions	Fundamental Functions				
	$\tilde{f}_1(x_1,x_2)$	$\tilde{f}_2(x_1,x_2)$	$\tilde{f}_3(x_1,x_2)$	$\tilde{f}_4(x_1,x_2)$	$\tilde{f}_5(x_1,x_2)$
SSSS	$x_1x_2(x_1-a)(x_2-b)$	$x_1x_2(x_1-a)(x_2-b)$	$x_1x_2(x_1-a)(x_2-b)$	$x_1x_2(x_1-a)(x_2-b)$	$x_1x_2(x_1-a)(x_2-b)$
SCSS	$x_1x_2(x_1-a)(x_2-b)$	$x_1x_2(x_1-a)(x_2-b)$	$x_1x_2(x_1-a)^2(x_2-b)$	$x_1x_2(x_1-a)(x_2-b)$	$x_1x_2(x_1-a)(x_2-b)$
SCSC	$x_1x_2(x_1-a)(x_2-b)$	$x_1x_2(x_1-a)(x_2-b)$	$x_1^2x_2(x_1-a)^2(x_2-b)$	$x_1x_2(x_1-a)(x_2-b)$	$x_1x_2(x_1-a)(x_2-b)$
SSSF	$x_2(x_1-a)(x_2-b)$	$x_2(x_1-a)(x_2-b)$	$x_2(x_1-a)(x_2-b)$	$x_2(x_1-a)(x_2-b)$	$x_2(x_1-a)(x_2-b)$
SFSF	$x_2(x_2-b)$	$x_2(x_2-b)$	$x_2(x_2-b)$	$x_2(x_2-b)$	$x_2(x_2-b)$
SCSF	$x_2(x_1-a)(x_2-b)$	$x_2(x_1-a)(x_2-b)$	$x_2(x_1-a)^2(x_2-b)$	$x_2(x_1-a)(x_2-b)$	$x_2(x_1-a)(x_2-b)$
CCCC	$x_1x_2(x_1-a)(x_2-b)$	$x_1x_2(x_1-a)(x_2-b)$	$x_1^2x_2^2(x_1-a)^2(x_2-b)^2$	$x_1x_2(x_1-a)(x_2-b)$	$x_1x_2(x_1-a)(x_2-b)$
SSCC	$x_1x_2(x_1-a)(x_2-b)$	$x_1x_2(x_1-a)(x_2-b)$	$x_1^2x_2(x_1-a)(x_2-b)^2$	$x_1x_2(x_1-a)(x_2-b)$	$x_1x_2(x_1-a)(x_2-b)$
SCCC	$x_1x_2(x_1-a)(x_2-b)$	$x_1x_2(x_1-a)(x_2-b)$	$x_1^2x_2(x_1-a)^2(x_2-b)^2$	$x_1x_2(x_1-a)(x_2-b)$	$x_1x_2(x_1-a)(x_2-b)$
CFCF	$x_2(x_2-b)$	$x_2(x_2-b)$	$x_2^2(x_2-b)^2$	$x_2(x_2-b)$	$x_2(x_2-b)$
SSFF	$x_2(x_1-a)$	$x_2(x_1-a)$	$x_2(x_1-a)$	$x_2(x_1-a)$	$x_2(x_1-a)$
CFSF	$x_2(x_2-b)$	$x_2(x_2-b)$	$x_2^2(x_2-b)$	$x_2(x_2-b)$	$x_2(x_2-b)$
CFFF	x_2	x_2	x_2^2	x_2	x_2
SFCS	$x_1x_2(x_2-b)$	$x_1x_2(x_2-b)$	$x_1x_2(x_2-b)^2$	$x_1x_2(x_2-b)$	$x_1x_2(x_2-b)$
CFCC	$x_1x_2(x_2-b)$	$x_1x_2(x_2-b)$	$x_1^2x_2^2(x_2-b)^2$	$x_1x_2(x_2-b)$	$x_1x_2(x_2-b)$
SFCC	$x_1x_2(x_2-b)$	$x_1x_2(x_2-b)$	$x_1^2x_2(x_2-b)^2$	$x_1x_2(x_2-b)$	$x_1x_2(x_2-b)$
FFCC	$x_1(x_2-b)$	$x_1(x_2-b)$	$x_1^2(x_2-b)^2$	$x_1(x_2-b)$	$x_1(x_2-b)$
CFCS	$x_1x_2(x_2-b)$	$x_1x_2(x_2-b)$	$x_1x_2^2(x_2-b)^2$	$x_1x_2(x_2-b)$	$x_1x_2(x_2-b)$
CSFF	$x_2(x_1-a)$	$x_2(x_1-a)$	$x_2^2(x_1-a)$	$x_2(x_1-a)$	$x_2(x_1-a)$
SFFF	x_2	x_2	x_2	x_2	x_2
FFFF	1	1	1	1	1

3. Numerical Results and Disscusions

In this section, the natural frequency parameters are obtained from the Rayleigh-Ritz method, presented here, and expressed in dimensionless form as $\lambda_n = \omega_n \frac{a^2}{h}\sqrt{\rho_{c/E_c}}$. Numerical calculations have been performed for different combinations of boundary conditions (SSSS, SCSS, SCSC, SSSF, SFSF, SCSF, CCCC, SSCC, SCCC, CFCF, SSFF, CFSF, CFFF, SFCS, CFCC, SFCC, FFCC, CFCS, CSFF, SFFF, FFFF). In the numerical calculations, Poisson's ratio $\vartheta = 0.38$ has been used. The FG nano-/microplate is made up of the following material properties: $\rho_c = 12.2 \times 10^3\ (\frac{\text{kg}}{\text{m}^3})$, $\rho_m = 1.22 \times 10^3\ \left(\frac{\text{kg}}{\text{m}^3}\right)$, $E_m = 1.44$ GPa, $E_c = 14.4$ GPa, and the small scale parameter is $l = 17.6 \times 10^{-6}$.

Table 2 shows a comparison study of the nondimensional natural frequency parameters ($\lambda_n = \omega_n \frac{a^2}{h}\sqrt{\rho_{c/E_c}}$) for a simply supported, FG, square nano-/microplate with those reported based on Mindlin plate theory by Thai and Choi [22]. The effect of the length scale parameter $\boldsymbol{l}$ and length-to-thickness ratio a/h on the first two nondimensional natural frequency parameters for simply supported, FG, rectangular nano-/microplates with a/b = 1 and different power-law indices are shown in Table 2.

From the results shown in Table 2, it can be observed that the present results, which were obtained by the Rayleigh-Ritz method, have greater values than those reported by Thai and Choi [22]. This is because in the Rayleigh-Ritz method, the admissible trial displacement and rotation functions that can satisfy the different boundary conditions at all edges of the plate are in the form of a finite polynomial series. Reducing the number of series terms decreases the degree of freedom of the plate and increases the stiffness and frequency parameter, in contrast with what was reported in Thai and Choi's work based on the Navier method (exact solution) [22]. Moreover, the different distribution of shear stress and rotary inertia in the thickness direction led to differences in the gained results, which are explained by the exponential, trigonometric, and first-order shear deformation plate theories. The results in Table 2 show that there is a good agreement between the present results and those of Thai and Choi [22].

Tables 3 and 4 show the effect of different boundary conditions, power-law index (g = 0, 1, and 10) and aspect ratios (a/b = 0.2, 0.5, and 1) on the dimensionless natural frequency ($\lambda_n = \omega_n \frac{a^2}{h}\sqrt{\rho_{c/E_c}}$) of FG, rectangular nano-/microplates using the exponential and trigonometric shear deformation plate theories. From the results presented in Tables 3 and 4, it can be observed that an increasing aspect ratio (a/b) leads to an increase in the dimensionless natural frequency parameters because decreasing the width of a plate with a constant length decreases the degrees of freedom of the plate and increases the stiffness.

Table 2. Comparison of nondimensional natural frequency of an FG nano-/microplate with all edges simply supported

a/h	l	λ_n	$g=0$			$g=1$			$g=10$		
			TSDT	ESDT	Ref. [22]	TSDT	ESDT	Ref. [22]	TSDT	ESDT	Ref. [22]
5	0	λ_1	5.48130	5.48140	5.38710	4.99490	4.99510	4.87440	5.66210	5.66230	5.58180
		λ_2	12.1209	12.1214	11.6717	10.9028	10.9035	10.7905	12.2316	12.2316	11.9931
	17.6×10^{-6}	λ_1	11.2690	11.2692	11.1311	11.2779	11.2784	4.0451	11.2364	11.2364	11.1666
		λ_2	23.9416	23.9418	23.7023	23.8609	23.8615	23.6723	23.8985	23.8987	23.7146
10	0	λ_1	6.21220	6.21220	5.93010	5.39620	5.39630	5.26970	5.13090	5.13120	5.09030
		λ_2	14.2254	14.2256	14.0893	12.7138	12.7139	12.6460	14.6621	14.6625	14.6464
	17.6×10^{-6}	λ_1	12.9139	12.9143	12.6360	12.6693	12.6693	12.4128	12.7405	12.7409	12.7302
		λ_2	29.6572	29.6576	29.4588	29.1949	29.1953	29.1174	30.0109	30.0113	29.6008
20	0	λ_1	6.35950	6.35960	6.09970	5.55870	5.5590	5.38800	6.56880	6.56910	6.38370
		λ_2	15.1465	15.1466	15.0319	13.4209	13.4210	13.3192	15.8744	15.8748	15.7108
	17.6×10^{-6}	λ_1	13.4285	13.4287	13.1786	13.2017	13.2020	12.8871	13.3998	13.3999	13.3030
		λ_2	32.5074	32.4947	32.4952	32.2374	31.6689	31.6689	31.6012	32.6132	32.6133

Table 3. Comparison of the fundamental nondimensional natural frequency parameter for SSSS, SCSS, SCSC, SSSF, SFSF, SCSF, CCCC, SSCC, SFCC, and FFCC, FG, square nano-/microplates for different aspect ratios and power-law index values

B.Cs.	a/b	TSDT			ESDT		
		$g=0$	$g=1$	$g=10$	$g=0$	$g=1$	$g=10$
SSSS	0.2	6.74260	6.70330	7.03750	6.74270	6.70340	7.03770
	0.5	7.92210	7.85740	9.77850	7.92220	7.85750	9.77880
	1	12.9141	12.8691	12.9402	12.9143	12.8693	12.9404
SCSS	0.2	6.76440	6.72160	7.05530	6.76450	6.72190	7.05570
	0.5	8.46420	5.76960	9.38480	8.46440	5.76980	9.38490
	1	14.3211	14.0617	14.7463	14.3214	14.0618	14.7465
SCSC	0.2	6.79180	6.74500	7.07760	6.79230	6.74540	7.07760
	0.5	15.6683	14.8162	15.6274	15.6684	14.8164	15.6274
	1	17.7941	17.3798	18.1385	17.7942	17.3800	18.1387
SSSF	0.2	1.10260	1.09340	1.12500	1.10290	1.09390	1.12700
	0.5	8.24740	8.34450	8.72150	8.24750	8.34450	8.72160
	1	8.34410	8.24750	8.72150	8.34450	8.24750	8.72160
SFSF	0.2	0.25680	0.24870	0.27090	0.25730	0.24870	0.27100
	0.5	1.70760	1.53900	1.78350	1.70780	1.53100	1.78370
	1	7.28010	7.19290	7.51360	7.28030	7.19320	7.51420
SCSF	0.2	2.77230	2.71550	2.79740	2.77240	2.71570	2.79750
	0.5	4.32500	4.25510	4.40540	4.32510	4.25520	4.40560
	1	9.17270	9.04800	9.21430	9.17290	9.04810	9.21430
CCCC	0.2	14.8817	14.4513	15.0081	14.8819	14.4513	15.0082
	0.5	15.7562	15.3826	15.9753	15.7562	15.3828	15.9753
	1	23.4676	2.35710	23.9911	23.4679	2.35750	23.9918
SSCC	0.2	10.3518	10.1382	10.5238	10.3519	10.1382	10.5243
	0.5	11.2156	10.9700	11.4295	11.2156	10.9700	11.4301
	1	17.2500	16.8890	17.3994	17.2510	16.8890	17.3995
SFCC	0.2	2.82760	2.76970	2.85210	2.82770	2.76970	2.85220
	0.5	4.98240	4.88110	5.04160	4.98250	4.88120	5.04160
	1	13.0364	12.7611	13.1615	13.0365	12.7617	13.1621
FFCC	0.2	2.48450	2.42670	2.50750	2.48490	2.42680	2.50770
	0.5	3.12170	3.05580	3.14700	3.12160	3.05610	3.14900
	1	5.25760	5.18070	5.29150	5.25770	5.18080	5.29150

Table 4. Comparison of the fundamental nondimensional natural frequency parameter for CFCS, CFCF, SSFF, CFSF, CFFF, SCCC, CFCC, SFCS, CSFF, SFFF, and FFFF, FG, square nano-/microplates for different aspect ratios and power-law index values.

B.C	a/b	TSDT			ESDT		
		$g=0$	$g=1$	$g=10$	$g=0^*$	$g=1$	$g=10$
CFCS	0.2	1.33890	1.31710	1.35290	1.33920	1.31750	1.35310
	0.5	4.99810	4.89340	5.05700	4.99820	4.89360	5.05720
	1	17.7295	17.3940	17.8126	17.7298	17.3941	17.8132
CFCF	0.2	0.65660	0.69230	0.65800	0.65680	0.69230	0.65900
	0.5	4.27970	4.18690	4.32290	4.28060	4.18700	4.32290
	1	19.7784	16.8847	19.8914	19.7786	16.8847	19.8915
SSFF	0.2	0.54950	0.54510	0.20700	0.55020	0.54510	0.20740
	0.5	1.37250	1.36100	1.40500	1.37260	1.36300	1.40520
	1	2.83340	2.78790	2.95380	2.83330	2.78790	2.95410
CFSF	0.2	0.43440	0.41960	0.44380	0.43520	0.42000	0.44400
	0.5	2.85180	2.78050	2.89660	2.85190	2.78050	2.89690
	1	11.7223	11.4958	11.8645	11.7224	11.4962	11.8647
CFFF	0.2	0.10220	0.09840	0.19550	0.10260	0.09900	0.19600
	0.5	0.66530	0.64780	0.67290	0.66570	0.64800	0.67300
	1	2.73140	2.67270	2.84260	2.73150	2.67270	2.84280
SCCC	0.2	14.7612	14.4490	14.9706	14.7614	14.4491	14.9707
	0.5	15.3964	15.0343	15.6270	15.3964	15.0347	15.6274
	1	2.22150	19.7427	20.3358	20.2216	19.7427	20.3359
CFCC	0.2	2.89300	2.83310	2.91670	2.89300	2.83320	2.91680
	0.5	5.93560	5.89910	5.98900	5.93590	5.81000	5.98950
	1	18.1151	17.7508	18.1563	18.1155	17.7509	18.1564
SFCS	0.2	1.21040	1.19590	1.22990	1.21090	1.19640	1.23070
	0.5	3.82210	3.75200	3.90450	3.82210	3.75220	3.90480
	1	12.4761	12.2398	12.5124	12.4766	12.2400	12.5125
CSFF	0.2	0.60400	0.59610	0.60870	0.60450	0.59630	0.60808
	0.5	1.74180	1.73000	1.78730	1.74190	1.73100	1.78730
	1	4.37990	4.35090	4.44600	4.38030	4.35090	4.44620
SFFF	0.2	0.08740	0.08430	0.08800	0.08780	0.08440	0.08840
	0.5	0.57890	0.55210	0.58840	0.57920	0.55230	0.58860
	1	2.17170	2.04140	2.81390	2.17190	2.04150	2.81410
FFFF	0.2	0.03750	0.03400	0.03790	0.03750	0.03430	0.03810
	0.5	0.33190	0.32070	0.34800	0.33190	0.32080	0.34860
	1	1.21410	1.17150	1.22510	1.21460	1.17160	1.22530

As the results show in Tables 2–4, the effect of the power-law index on dimensionless natural frequencies is very interesting. It is observed that increasing the power-law index value initially decreases, reaches a minimum, and then increases the frequency. This is because decreasing or increasing the dimensionless natural frequency depends on the kind of material researchers choose to study. For example, Matsunga [5] presented the free vibration and stability of FG plates according to a 2D, higher-order deformation theory in which the frequency parameter decreases with an increase in the power-law index. On the other hand, Thai and Choi [22] analyzed size-dependent, FG, Kirchhoff and Mindlin plate models based on a modified couple stress theory. Their results show that the frequency parameter decreases first and then rises. This phenomenon could be due to the fact that the frequency parameter of FG materials are dependent on both Young's modulus (Young's modulus $\propto$ plate rigidity) and density (density $\propto$ plate softening). In the presented material research, and similar to the results reported by Thai and Choi [22], with an increase in the power-law index, the dimensionless natural frequency decreases first and then rises because an increase in the power-law index in this research's material caused Young's modulus and density to decrease. A reduction in the Young's modulus, consequently, caused the plates rigidity and frequency parameter to decrease. However, a decrease in the density leads to an increase in the frequency parameter. So, first, the effect of the Young's modulus is greater than the effect of density on the frequency parameter; consequently, the dimensionless natural frequency first decreases. But after reaching a minimum, the effect of the density becomes greater than the effect of Young's modulus, and it causes the dimensionless natural frequency to increase. By comparing the obtained dimensionless natural frequencies of the different boundary conditions that are shown in Tables 2–6, it was found that the dimensionless natural frequencies increase as the degrees of freedom of the plate decrease (increasing the geometric constraints on the edges of the plate). Because of the decreased degree of freedom at each edge of the rectangular plate, the plate

gets stiffer, leading to increased dimensionless natural frequencies.

Tables 5 and 6 show the effect of the different boundary conditions and length-to-thickness ratios (a/h = 5, 8, 15, and 20) on the 3 first dimensionless natural frequencies ($\lambda_n = \omega_n \frac{a^2}{h}\sqrt{\rho_{c/E_c}}$) of homogeneous, rectangular nano-/microplates using the exponential and trigonometric shear deformation plate theories. From the results in Tables 5 and 6, it can be found that, with an increase in the length-to-thickness ratio (constant length and thickness decreases), the dimensionless natural frequency increases. From these results, it can be seen that if the thickness increases, the effective stiffness and effective mass of the plate increase, but the growth of the effective stiffness is greater than the effective mass, so the natural frequency of the nano-/microplate increases.

As shown in Table 2, it can be found that the dimensionless natural frequency of nano-/microplates according to couple stress theory is greater than the dimensionless natural frequency of the plate, due to classical linearly elastic continuum mechanics ($l = 0$). This is because the potential energy of linearly elastic continuum mechanics is only defined by a function of the strain tensor in the classical exponential and trigonometric shear deformation plate theories.

Table 5. Comparison of the three first nondimensional natural frequency parameters for SSSS, SCSS, SCSC, SSSF, SFSF, SCSF, CCCC, SCCC, CFCC, SSCC, and SFCC, homogeneous, square nano-/microplates for different length-to-thickness ratios (g = 0, a/b = 1, $a = 10l$)

B.C	a/h	TSDT			ESDT		
		First mode	Second mode	Third mode	First mode	Second mode	Third mode
SSSS	5	7.51870	17.3733	19.0881	7.51870	17.3734	19.0885
	8	10.0573	24.4701	27.7967	10.0574	2404702	27.7967
	15	16.5254	41.5901	48.3785	16.5255	41.5901	48.3788
	20	21.4144	54.2730	63.4540	21.4145	54.2770	63.4543
SCSS	5	8.78180	19.0883	19.7049	8.78180	19.0885	19.7053
	8	12.0816	28.6735	28.9464	12.0817	28.6739	28.9468
	15	20.1517	49.9971	50.3354	20.1517	49.9104	50.3357
	20	26.1871	65.4489	65.9540	26.1877	65.4489	65.9542
SCSC	5	10.4071	19.0814	19.0949	10.4078	19.0816	19.0952
	8	14.8677	30.0424	30.4398	14.8677	30.0424	30.4398
	15	24.8474	53.0401	57.2942	24.8475	53.0401	57.2944
	20	32.9207	68.8501	76.2986	32.9207	68.8502	76.2987
SSSF	5	5.61190	12.1597	12.3623	5.61230	12.1604	12.3624
	8	7.75880	17.8060	19.4560	7.75900	17.8130	19.4566
	15	12.8753	30.6762	36.4799	12.8755	30.6762	36.4812
	20	16.7024	40.1169	48.6415	16.7025	401171	48.6416
SFSF	5	4.50840	7.07060	8.97390	4.50870	7.07110	8.97430
	8	6.15490	9.86400	14.3589	6.15520	9.86410	14.3589
	15	16.2031	16.5390	26.9227	16.2031	16.5391	26.9229
	20	13.2273	21.4775	35.8966	13.2281	21.4781	35.8972
SCSF	5	5.61260	12.1599	12.3625	5.61270	12.1609	12.3628
	8	7.73590	17.8168	19.4568	7.73590	17.8170	19.4569
	15	12.8754	30.6763	36.4815	12.8759	30.6764	36.4815
	20	16.7027	40.1171	48.6419	16.7029	40.1173	48.6419
CCCC	5	33.6435	36.5426	50.7359	33.6441	36.5427	50.7356
	8	19.2698	19.5999	27.0412	19.2698	19.6007	27.0417
	15	33.6437	36.5425	50.7354	33.6441	36.5427	50.7359
	20	44.6753	48.5931	67.4057	44.6753	48.5932	67.4061
SCCC	5	11.6715	19.0884	19.0905	11.6717	19.0848	19.0906
	8	16.9500	30.5411	30.5487	16.9560	30.5417	30.5488
	15	28.6675	57.1772	57.2543	28.6683	57.1773	57.2544
	20	37.7139	76.3458	82.0034	37.7139	76.3459	82.0035
CFCC	5	10.1566	12.1604	15.0731	10.1567	12.1604	15.0734
	8	14.9629	19.4554	22.2904	14.9637	19.4566	22.2911
	15	26.0903	36.4809	38.8571	26.0918	36.4812	38.8576
	20	34.2044	48.6405	50.9229	34.2048	48.6416	50.9237
SSCC	5	10.2615	19.0878	20.5756	10.2617	19.0885	20.5762
	8	14.1480	30.1797	30.5415	14.4481	30.1799	30.5416
	15	24.4789	52.4607	57.2644	24.4775	52.4612	57.2654
	20	31.9134	68.7304	76.3535	31.9135	68.7305	76.3539
SFCC	5	7.63620	12.1697	16.9177	7.63680	12.1604	16.9181
	8	10.8778	19.4565	19.6766	10.8800	19.4566	19.6768
	15	18.5530	34.0324	36.4805	18.5534	34.0332	36.4812
	20	24.2066	44.5387	48.6414	24.2071	44.5388	48.6416

Table 6. Comparison of the three first nondimensional natural frequency parameter for SSCC, SFCC, FFCC, CFCS, SFCS, CSFF, CFCF, SSFF, CFSF, CFFF, SFFF, and FFFF, homogeneous, square nano-/microplates for different length-to-thickness ratios ($g = 0$, $a/b = 1$, $a = l$)

B.C	a/h	TSDT			ESDT		
		First mode	Second mode	Third mode	First mode	Second mode	Third mode
SSCC	5	10.2615	19.0878	20.5756	10.2617	19.0885	20.5762
	8	14.1480	30.1797	30.5415	14.4481	30.1799	30.5416
	15	24.4789	52.4607	57.2644	24.4775	52.4612	57.2654
	20	31.9134	68.7304	76.3535	31.9135	68.7305	76.3539
SFCC	5	7.63620	12.1697	16.9177	7.63680	12.1604	16.9181
	8	10.8778	19.4565	19.6766	10.8800	19.4566	19.6768
	15	18.5530	34.0324	36.4805	18.5534	34.0332	36.4812
	20	24.2066	44.5387	48.6414	24.2071	44.5388	48.6416
FFCC	5	3.09160	7.74880	10.1395	3.09180	7.74920	10.1397
	8	4.38650	12.3987	13.6710	4.38680	12.3987	13.6711
	15	7.59480	22.8321	23.2474	7.59510	22.8323	23.2475
	20	9.96240	29.6263	30.9967	9.96270	29.6265	30.9967
CFCS	5	9.27710	12.1604	16.9177	9.92720	12.1604	16.9181
	8	14.6350	19.4550	20.0741	14.6355	19.4566	20.0742
	15	25.5664	34.6873	36.4810	25.5669	34.6875	36.4812
	20	33.5368	45.3788	48.6414	33.5370	45.3792	48.6416
SFCS	5	7.32940	12.0537	16.9175	7.33010	12.0543	16.9181
	8	10.4110	17.1287	19.4562	10.4140	17.1289	19.4566
	15	17.7661	29.1804	36.2807	17.7667	29.1811	36.2810
	20	23.1911	38.0744	48.6409	23.1912	38.0750	48.6416
CSFF	5	2.51760	7.74920	10.1395	2.51770	7.74920	10.1397
	8	3.60220	10.8308	12.3984	3.60230	10.8310	12.3987
	15	6.29700	17.9114	23.2474	6.29800	17.9114	23.2475
	20	8.28140	23.2027	30.9965	8.28150	23.2027	30.9967
CFCF	5	8.97350	11.0581	16.5346	8.97390	11.0593	16.5349
	8	14.3237	14.3596	16.3444	14.3243	14.3596	16.3444
	15	26.0234	26.9226	28.4434	26.0234	26.9226	28.4434
	20	32.7453	35.8962	37.2508	32.7453	35.8962	37.2508
SSFF	5	1.60500	7.32850	8.11560	1.60520	7.32850	8.1157
	8	2.27180	9.77330	11.7010	2.27190	9.77340	11.7012
	15	3.91660	15.8020	20.2374	3.91690	15.8028	20.2377
	20	5.12450	20.3741	26.4930	5.12480	20.3743	26.4931
CFSF	5	6.83580	8.83300	15.5240	6.83580	8.83300	15.5240
	8	9.76190	12.6404	14.3587	9.76200	12.6404	14.3589
	15	16.7449	21.5320	26.9226	16.7452	21.5324	26.9229
	20	21.8871	28.0662	35.8968	21.8875	28.0669	38.8972
CFFF	5	1.65510	3.33970	7.96540	1.65540	3.34000	7.96570
	8	2.28730	5.34350	5.71790	2.28760	5.34400	5.71810
	15	3.88520	10.0199	10.0614	3.88530	10.0199	10.0615
	20	5.07170	13.2334	13.3599	5.07200	13.2335	13.3599
SFFF	5	0.75970	1.48690	3.54460	0.76020	1.48690	3.54470
	8	1.27650	2.93840	3.16750	1.27670	2.93870	3.16780
	15	0.06170	0.53760	0.68850	2.15720	5.55500	5.57400
	20	0.10610	0.56070	1.34340	5.07200	7.32740	7.41210
FFFF	5	0.45090	0.60490	1.44230	0.45110	0.60490	1.44240
	8	0.51910	1.19480	1.28640	0.51920	1.19490	1.28630
	15	0.87680	2.27960	2.26100	0.87710	2.26020	2.26600
	20	2.06410	4.34430	4.39290	2.06430	4.34430	4.39310

4. Conclusion

The free vibration of size-dependent, rectangular, FG, nano-/microplates was analyzed based on nonlinear shear deformation plate theories using modified couple stress theory. The modified couple stress theory contains one material-length scale parameter, and it can also be degenerated to the classical FG, rectangular plate by setting the material-length scale parameter equal to zero. Equations of motion for free vibration can be found through an implementation of the Rayleigh-Ritz method, which may satisfy any combination of boundary conditions, including: SSSS, SCSS, SCSC, SSSF, SFSF, SCSF, CCCC, SSCC, SCCC, CFCF,

SSFF, CFSF, CFFF, SFCS, CFCC, SFCC, FFCC, CFCS, CSFF, SFFF, and FFFF. Material properties were assumed to change continuously through the thickness according to a power-law distribution. A comparison of the present results with those reported in the literature for size-dependent, rectangular, FG nano-/microplates illustrated the high accuracy of the present study. This research shows the effects of variations of the length scale parameter, length-to-thickness ratio, power-law index, and the aspect ratio as well as different boundary conditions on the free vibration of a size-dependent, rectangular, FG nano-/microplate.

By looking into the present results, the following points may be concluded:

- Increasing the aspect ratio (a/b) causes an increase in the dimensionless natural frequency.
- With an increase in the power-law index, the dimensionless natural frequency decreases first and then increases.
- The dimensionless natural frequencies of the size-dependent, rectangular nano-/microplate increase with a decreasing degree of freedom at the boundary conditions of the plate.
- With an increasing length-to-thickness ratio (constant length and thickness decreases), the dimensionless natural frequency increases.
- The transverse shear and rotary inertia have a dissimilar effect in the exponential and trigonometric shear deformation plate theories.
- The dimensionless natural frequency of the FG, rectangular nano-/microplate based on the couple stress theory is more than the dimensionless natural frequency of the FG, calssical plate.

All analytical results presented here can be provided to other research groups of a reliable source to compare their analytical and numerical solutions.

Acknowledgments

The authors gratefully acknowledge the funding by Arak University, under Grant No. 95/8589.

References

[1] Yang FA, Chong AC, Lam DC, Tong P. Couple stress based strain gradient theory for elasticity. *Int J Solides Struct* 2002; 39: 2731-2743.

[2] Eringen AC. Nonlocal polar elastic continua. *Int J Eng Sci* 1972; 10: 1-16.

[3] Nix WD, Gao H. Indentation size effects in crystalline materials: a law for strain gradient plasticity. *J Mech Phys Solids* 1998; 46: 411-425.

[4] Lu C, Wu D, Chen W, Non-linear responses of nano-scale FGM films including the effects of surface energies. *IEEE Trans Nanotechnol* 2011; 10(6); 1321–1327.

[5] Matsunaga H. Free vibration and stability of functionally graded plates according to a 2- graded plates according to a 2-D higher-order deformation theory. *Compos Struct* 2008; 82; 499-512.

[6] Salehipour H, Nahvi H, Shahidi AR. Exact closed-form free vibration analysis for functionally graded micro/nano plates based on modified couple stress and three-dimensional elasticity theories. *Compos Struct* 2015; 124: 283-291.

[7] Ansari R, Faghih-Shojaei M, Mohammadi V, Gholami R, Darabi MA. Nonlinear vibrations of functionally graded Mindlin microplates based on the modified couple stress theory. *Compos Struct* 2014; 114: 124-134.

[8] Kim J, Reddy JN. Analytical solutions for bending, vibration, and buckling of FGM plates using a couple stress-based third-order theory. *Compos Struct* 2013; 103: 86-98.

[9] Thai H-T, Vo TP. A size-dependent functionally graded sinusoidal plate model based on a modified couple stress theory. *Compos Struct* 2013; 96: 376-383.

[10] Shaat M, Mahmoud FF, Gao X-L, Faheem AF. Size-dependent bending analysis of Kirchhoff nanoplates based on a modified couple-stress theory including surface effects. *Int J Mech Sci* 2014; 79: 31-37.

[11] Lou J, He L. Closed-form solutions for nonlinear bending and free vibration of functionally graded microplates based on the modified couple stress theory. *Compos Struct* 2015; 131: 810-820.

[12] He L, Lou J, Zhang E, Wang Y, Bai Y. A size-dependent four variable refined plate model for functionally graded microplates based on modified couple stress theory. *Compos Struct* 2015; 130: 107-115.

[13] Zhang B, He Y, Liu D, Shen L, Lei J. An efficient size-dependent plate theory for bending, buckling and free vibration analyses of functionally graded microplates resting on elastic foundation. *Appl Math Model* 2015; 39(13): 3814-3845.

[14] Lou J, He L, Du J. A unified higher order plate theory for functionally graded microplates based on the modified couple stress theory. *Compos Struct* 2015; 133: 1036-1047.

[15] Thai H-T, Kim S-E. A size-dependent functionally graded Reddy plate model based on a modified couple stress theory. *Compos Part B: Eng* 2013; 45(1): 1636-1645.

[16] Gupta A, Jain NK, Salhotra R, Joshi PV. Effect of microstructure on vibration characteristics of partially cracked rectangular plates based on a

modified couple stress theory. *Int J Mech Sci* 2015; 100: 269-282.

[17] Li YS, Pan E. Static bending and free vibration of a functionally graded piezoelectric microplate based on the modified couple-stress theory, *Int J Eng Sci* 2015; 97: 40-59.

[18] Nguyen HX, Nguyen TN, Abdel-Wahab M, Bordas SPA, Nguyen-Xuan H, Vo TP. A refined quasi-3D isogeometric analysis for functionally graded microplates based on the modified couple stress theory. *Comput Meth Appl Mech Eng* 2017; 313: 904-940.

[19] Lei J, He Y, Zhang B, Liu D, Shen L, Guo S. A size-dependent FG micro-plate model incorporating higher-order shear and normal deformation effects based on a modified couple stress theory. *Int J Mech Sci* 2015; 104: 8-23.

[20] Jandaghian AA, Rahmani O. Vibration analysis of functionally graded piezoelectric nanoscale plates by nonlocal elasticity theory: An analytical solution. *Superlattices Microstructures* 2016; 100: 57-75.

[21] Şimşeka M, Aydınc M. Size-dependent forced vibration of an imperfect functionally graded (FG) microplate with porosities subjected to a moving load using the modified couple stress theory. *Compos Struct* 2017; 160: 408-421.

[22] Thai HT, Choi DH. Size-dependent functionally graded Kirchhoff and Mindlin plate models based on a modified couple stress theory. *Compos Struct* 2013; 95; 142-153.

[23] Khorshidi K, Asgari T, Fallah A. Free vibrations analaysis of functionally graded rectangular nanoplates based on nonlocal exponential shear deformation theory. *Mech Adv Compos Struct* 2016; 2(2): 79-93.

[24] Khorshidi K, Fallah A. Buckling analysis of functionally graded rectangular nano-plate based on nonlocal exponential shear deformation theory. *Int J Mech Sci* 2016; 113: 94-104.

[25] Khorshidi K, Khodadadi M. Precision Closed-form Solution for Out-of-plane Vibration of Rectangular Plates via Trigonometric Shear Deformation Theory. *Mech Adv Compos Struct* 2016; 3(1): 31-43.

[26] Reddy JN, Kim J. A nonlinear modified couple stress-based third-order theory of functionally graded plates. *Compos Struct* 2012; 94(3);1128-1143.

[27] Simsek M, Reddy JN. Bending and vibration of functionally graded microbeams using a new higher order beam theory and the modified couple stress theory. *Int J Eng Sci* 2013; 64; 37–53.

[28] Jung WY, Han SCH, Park WT. A modified couple stress theory for buckling analysis of S-FGM nanoplates embedded in Pasternak elastic medium. *Compos Part B* 2014; 60; 746–56.

[29] Jung WY, Park WT, Han SCH. Bending and vibration analysis of S-FGM microplates embedded in Pasternak elastic medium using the modified couple stress theory. *Int J Mech Sci* 2014; 87;150–62.

[30] Ramu I, Mohanty SC. Study on free vibration analysis of rectangular plate structures using finite element method. *Procedia Eng* 2012; 31(38):2758-66.

[31] Gospodinov G, Ljutskanov D. The boundary element method applied to plates. *Appl Math Model* 1982; 6(4); 237-244.

[32] Chang, AT. An improved finite difference method for plate vibration. International Journal for Numerical Methods in Engineering 1972; 5(2); 289-296.

[33] Liew K M, Liu FL. Differential quadrature method for vibration analysis of shear deformable annular sector plates. *J Sound Vib* 2000; 230(2); 335-356.

[34] Chu F, Wang L, Zhong Z, He J. Hermite radial basis collocation method for vibration of functionally graded plates with in-plane material inhomogeneity. *Comput Struct* 2014; 142; 79-89.

[35] Saadatpour MM, Azhari M. The Galerkin method for static analysis of simply supported plates of general shape. *Comput Struct* 1998; 69(1); 1-9.

[36] Reddy JN. Nonlocal theories for bending, buckling and vibration of beams. *Int J Eng Sci* 2007; 45(2); 288-307.

[37] Khorshidi K. Effect of hydrostatic pressure on vibrating rectangular plates coupled with fluid. *Sci Iranica. Trans A: Civil Eng* 2010; 17(6): 415–29.

[38] Hosseini-Hashemi Sh, Khorshidi K, Payandeh H. Vibration analysis of moderately thick rectangular plates with internal line support using the Rayleigh-Ritz approach. *Sci Iranica. Trans B: Mech Eng* 2009; 16(1): 22-39,

[39] Khorshidi K, Bakhsheshy A. Free Natural Frequency Analysis of an FG Composite Rectangular Plate Coupled with Fluid using Rayleigh–Ritz Method. *Mech Adv Compos Struct* 2014; 1(2): 131-143.